A Paleosol Identified By Optically Stimulated Luminescence Dating in the Excavation of a Tank in Agreste of Pernambuco State, NE Brazil

Rodrigo Ranulpho[1] · Viviane Khoury Asfora[2] · Gelson Luís Fambrini[1,3] · Edison Vicente Oliveira[1,3] · Jorge Luiz Lopes da Silva[4] · Marcelo Metri Corrêa[5] · Alex de Souza Moraes[6] · Ygor Jacques Agra Bezerra da Silva[7] · João Adauto de Souza Neto[1,3] · Virgínio Henrique de Miranda Lopes Neumann[1,3]

Abstract

Sediments from a tank excavation in the municipality of Fazenda Nova, Pernambuco, were analyzed to determine the origin and dating of two calcrete levels found at the base and the top of the profile. The goal of the study was to generate a lithostratigraphic description and establish a timeline of these calcrete levels. The excavation consisted of a trench with dimensions of 1.5 m on each side and 1.65 m in depth, in which nine units (R1.1 to R1.9) were described from base to top. Fossil fragments were discovered at levels R1.2 and R1.6, which also showed higher calcium oxide (CaO) content, confirming their classification as calcrete levels. Four samples were collected for optically stimulated luminescence (OSL) testing. OSL analysis revealed that the oldest samples at the base of the profile were associated with time intervals between $45,058 \pm 3,093$ years (R1.2), corresponding to the conglomeratic calcrete level containing bone fragments from the mammalian megafauna. The sediments from the middle to the top of the profile (R1.4 = $7,078 \pm 401$; R1.6 = $4,194 \pm 223$; R1.7 = $3,823 \pm 339$) were found to be more recent, with age differences between the oldest and youngest samples ranging from 38,000 to 42,000 years. There was an additional calcrete level of granular specification from the middle to the top (R1.6). Both calcrete levels were confirmed to be of pedogenetic origin. The most basal level, being older than 11,000 years, predates the Holocene age and is hence classified as a paleosol.

✉ Viviane Khoury Asfora
viviane.asfora@ufpe.br

Rodrigo Ranulpho
rodrigo.ranulpho@ufpe.br

Gelson Luís Fambrini
gelson.fambrini@ufpe.br

Edison Vicente Oliveira
edison.vicente@ufpe.br

Jorge Luiz Lopes da Silva
jluizlopess@gmail.com

Marcelo Metri Corrêa
marcelo.metri@ufape.edu.br

Alex de Souza Moraes
alex.moraes@ufrpe.br

Ygor Jacques Agra Bezerra da Silva
ygor.silva@ufrpe.br

João Adauto de Souza Neto
joao.souzant@ufpe.br

Virgínio Henrique de Miranda Lopes Neumann
virginio.neumann@ufpe.br

[1] Programa de Pós-Graduação em Geociências, Universidade Federal de Pernambuco, Av. da Arquitetura s/n, Cidade Universitária, 50740-550 Recife, PE, Brazil

[2] Departamento de Energia Nuclear, Universidade Federal de Pernambuco, Av. Professor Luis Freire, Cidade Universitária, Av. Professor Luis Freire, s/n, Cidade Universitária, 50730-120 Recife, PE, Brazil

[3] Departamento de Geologia, Universidade Federal de Pernambuco, Av. da Arquitetura, s/n, Cidade Universitária, Recife, PE, Brazil

[4] Laboratórios Integrados de Paleontologia e Espeleologia (LIPE), Museu de História Natural, Universidadde Federal de Alagoas. Avenida Amazonas, Avenida Amazonas, s/n, Al, Prado Maceió 57010-060, Brazil

[5] Universidade Federal do Agreste de Pernambuco, Avenida Bom Pastor, s/n, Boa Vista, Garanhuns, PE 55292-270, Brazil

[6] Departamento de Química, Universidade Federal Rural de Pernambuco, Avenida Dom Manoel de Medeiros, Dois Irmãos, Recife, PE 52171-900, Brazil

[7] Departamento de Agronomia, Universidade Federal Rural de Pernambuco, Avenida Dom Manoel de Medeiros, Dois Irmãos, Recife, PE 52171-900, Brazil

🌀 Springer

1 Introduction

Luminescence dating, especially when used for quaternary events, is a simple concept [1–3]. Optically Stimulated Luminescence (OSL) dating, a well-established technique, can determine deposition ages of sediments ranging from several decades to hundreds of thousands of years. Standard minerals like quartz and most feldspars possess the ability to absorb energy into their crystal structures; the stored energy level correlates with radiation exposure. This essentially forms a "clock", a fundamental aspect of all luminescence dating methods.

Luminescence dating plays a vital role in documenting the Quaternary period's dramatic environmental changes, marked by significant climate fluctuations, such as alternating warm, cold, dry, and humid conditions [4–7]. These shifts directly impact rock weathering and the ensuing erosion processes, resulting in the formation of eluvial, colluvial, and alluvial deposits [8]. These geomorphological structures, enclosing and overlaying batholiths and inselbergs, generate extensive sedimentary deposits comprising primary minerals from granitic rock and new secondary minerals.

In some parts of the landscape, these sediments settle in stratigraphic layers, marking the alternation between periods of tranquility and new deposition flows. Landscape stability promotes soil development and pedological interactions. In contrast, new climate inputs ignite gravitational flows like mudflows and debris flows, covering surfaces that have been exposed for an extended period [9, 10]. This process preserves the buried records of a former environment, referred to as paleosols [11].

The geomorphological changes, such as erosion and sediment transport, significantly affect the resetting of luminescence in minerals. Luminescence is achieved in mineral grains as a result of ionizing radiation and electron trapping during the formation of a rock's crystal structure. Exposure to light on soil surfaces, through erosion, and during sediment transport resets the luminosity of minerals. Following this, a new layer of sediment is deposited, concealing the previously exposed surface and preventing further exposure to solar radiation. With geological burial and continued exposure to ionizing radiation, free electrons are captured in charge defects within the grain's crystal lattice. Consequently, as the grains undergo further burial, they acquire luminescence through exposure to ionizing radiation [12–15].

The resetting and reacquisition of luminescence, prompted by environmental shifts, emphasize the versatility of OSL dating in numerous geoscientific disciplines. The use of OSL dating has seen a rise across various geological sciences. Feathers [16] highlighted the use of luminescence dating in archaeology, noting enhanced methodology and improved instrumentation that fortify its role as a chronological tool within the field. Carvalho et al. [17] employed the OSL method to identify the depositional age of Pleistocene and Holocene sediments. This enabled the distinction of the Barreiras Formation sediments, aged between 17 and 24 million years old. It was also determined that these sediments were deposited under the impact of the Cenozoic uplift in Northeast Brazil.

The first OSL dating experiments used green wavelength light beams to stimulate the OSL signal of quartz and feldspar. Subsequently, it was observed that the optimal wavelength for stimulating quartz was between blue light (~ 470 nm) and green light (~ 510 nm). Advances were made following the studies by Hütt et al. [18], which demonstrated that feldspar could be stimulated at room temperature. These studies identified infrared stimulated luminescence (IRSL) at wavelengths ranging from 0.8 to 2.5 μm. This discovery was surprising because existing physical models at the time suggested that infrared wavelengths would not provide enough energy to release electrons from deep traps. However, multiple comparisons with independent dating methods confirmed the validity of the IRSL technique. As a result of Hütt et al.'s research [18], OSL dating of feldspars became more cost-effective by using infrared light-emitting diodes instead of more expensive lasers [19].

The first published results of sedimentary dating using feldspar grains were presented by Duller [20] and Lamothe et al. [21]. However, quartz has generally been preferred for dating because it does not exhibit anomalous fading. Despite this, subsequent studies demonstrated the potential of feldspar dating by using a combination of thermally assisted IRSL readings to determine the accumulated dose. Advances in recent decades, along with new methods and discoveries [22–24], have significantly improved the reliability of dates obtained from feldspar OSL.

The purpose of this study is to use the OSL method to distinguish two calcrete levels in a dug pit in the Fazenda Nova region, Pernambuco, aiding in the discovery of a paleosoil. The Borborema Province, known for its intricate geological past involving Neoproterozoic units and substantial tectonic activities, encompasses this region. The province's current landscape is a testament to these times. Given its backdrop, the region is an optimal location for examining Quaternary sediments using OSL dating. This technique is key in piecing together the environmental and geological timelines of Northeast Brazil. Furthermore, the accurate dating and identification of paleosoils provide an invaluable perspective on aged soil formation processes, contributing significantly to the restoration of past landscapes. It also provides implications for future environmental and geological research in the vicinity.

2 Area Location

The study was conducted in the Fazenda Nova district, located within the municipality of Brejo da Madre de Deus, which is part of the Agreste mesoregion and the Vale do Ipojuca microregion in Pernambuco's central-eastern region. The district lies within the Borborema Plateau's geomorphological domain, nestled in the Pernambucan Interplateau Depression [25] (Fig. 1).

The excavation site is located in residual granite outcrops resembling inselbergs and tors. It is staged within a vast amphitheater, flanked by curved massifs that range from 600 to 900 m in altitude, including the Granito Serra do Quati and the Caruaru-Arcoverde Pluton, which open northeastward. Predominantly formed by Planosols [26], the area is characterized by pediments approximately 400 m high, intersected by intermittent and temporary dendritic drainages composing the Capibaribe River Watershed.

The locale is home to the Caatinga biome's dominant vegetation. The lower, hotter, and drier regions exhibit hyperxerophilic vegetation, while cooler and moister high-altitude areas display hypoxerophilic vegetation. The climate, classified as semi-arid with hot altitude and low latitude (Bsh) according to the Köppen classification, experiences less than 760 mm of annual rainfall, predominantly between March and May, with an average annual temperature exceeding 22 °C.

3 Geological Setting

The subject of our study is a rugged area of Pernambuco State. This location is situated in the Northeast region of Brazil, within the Central Domain (also known as the Transversal Zone) of the Borborema Province [27]. It is known for its hot and dry climate, which is characteristic of the tropics, with somewhat milder temperatures experienced during the rainy season. The excavation site is specifically located within a sediment deposit inside a tank, which is embedded in an outcrop of porphyritic granite within the Nova Pluton farm.
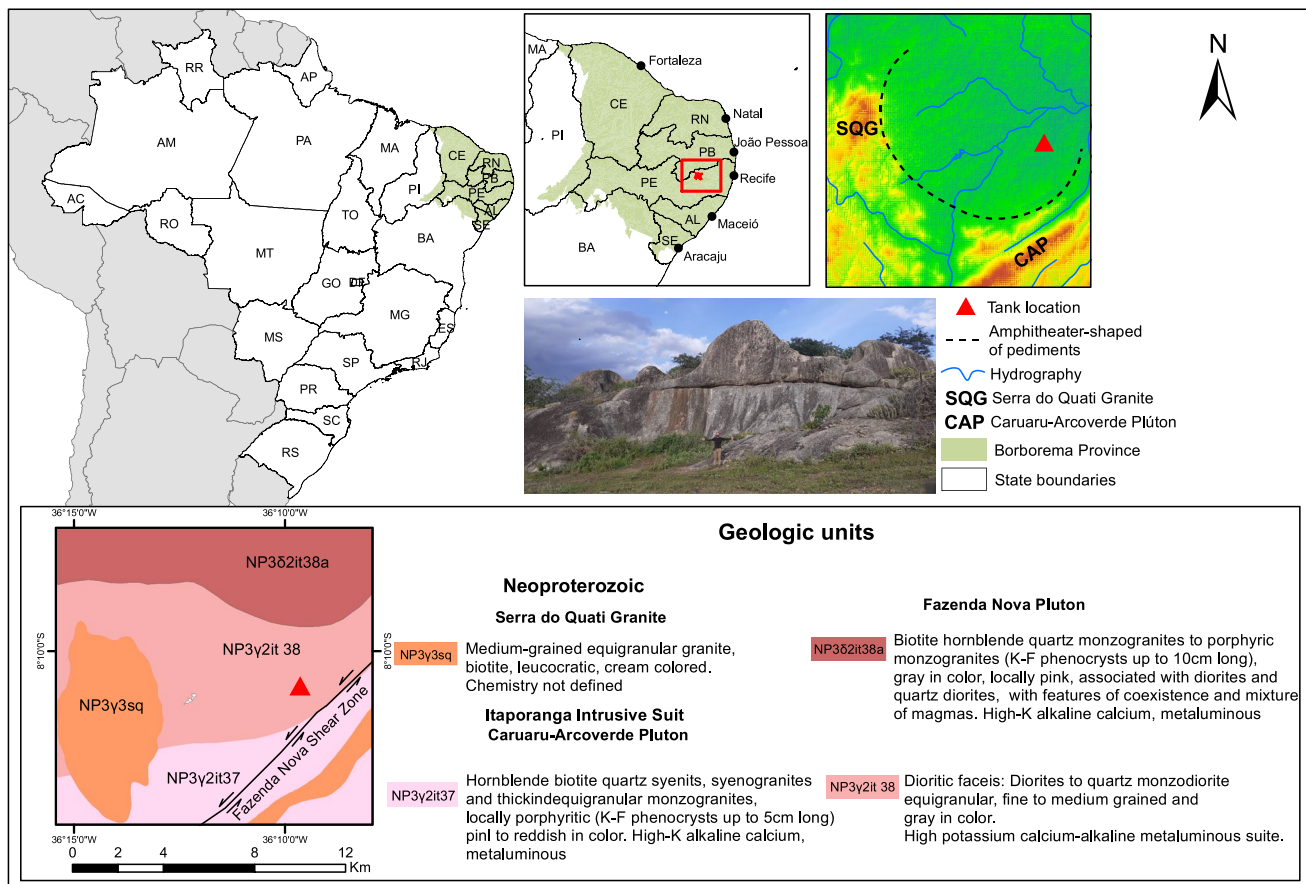

Fig. 1 Localization of study area and context of the local geology in municipality of Brejo da Madre de Deus, Pernambuco

Mariano et al. [28] describe the primary structural characteristics of the area. There is the Pernambuco Leste dextral strike-slip shear zone (ZCPE), which primarily runs east–west through the center of the sheet. Also, sinistral strike-slip zones branch from the ZCPE in a northeastern direction. These zones are notably found in the center and northern part of the sheet, specifically, the Fazenda Nova shear zone.

Several authors have proposed that the formation of the Borborema Province resulted from a multifaceted collisional process tied to the convergent movement of tectonic plates. This possibly incorporated the merging and accrual of microplates [29, 30].

This process likely culminated at the end of the Brasiliano event (580–540 Ma). Nevertheless, some authors view the Borborema Province as part of a larger orogen primarily formed in an intracontinental setting [31–33]. The study area features four Neoproterozoic (Ediacaran) geological units. Three of these belong to the Itaporanga Intrusive Suite, while one is a part of the Serra do Quati Granite (Fig. 1). The Itaporanga Intrusive Suite includes the Caruaru-Arcoverde Pluton, a prominent intrusive body in the Borborema Province, along with the porphyritic and dioritic facies of the Fazenda Nova Pluton [34, 35].

The Fazenda Nova Pluton includes two geologic units. The first is a dioritic facies, which encompasses fine-to-medium-grained, gray-colored diorites and equigranular monzodiorites with a high-potassium calcium-alkaline makeup. The second unit consists of biotite hornblende quartz monzonites and porphyritic monzogranites, featured by gray K-feldspar phenocrysts that might be up to 10 cm long and occasionally pink. They are combined with diorites and quartz diorites, displaying attributes of magma coexistence and mixing. This unit is defined as high-potassium, alkaline calcium, and metaluminous. The pluton's age, established through U-Pb dating, is 588 Ma [28].

The Caruaru-Arcoverde Pluton consists of hornblende biotite quartz syenites, syenogranites, and locally porphyritic, coarse inequigranular monzogranites. These are pink to reddish in color and feature microgranular enclaves of quartz diorite. They are high-K alkaline calcium and are metaluminous. According to Pb-Pb dating, they are approximately 591 ± 5 Ma and 587 ± 5 Ma old [28]. The Serra do Quati Granite is a medium-grained, leucocratic, cream-colored, equigranular biotite granite. However, its chemical composition remains undefined [28].

4 Materials and Methods

4.1 Description of the Sedimentological Profile

An excavation of the sedimentological profile was carried out in a tank situated in the Fazenda Nova district, PE. The tank, approximately elliptical in shape, measures around 15 ms long, 6 ms wide, and 2 m deep. The analysis of the sedimentological profile started from the bottom and progressed upwards, initiating with the saprolite, also known as the altered rock layer (R1.1): (R1.1) At the base of the profile, there is a level of altered rock (saprolite) that is approximately 30 cm thick (Fig. 2); (R1.2) Carbonate layer (conglomeratic calcrete), with bone fragments (megafauna); (R1.3) Clayey sand with gravel; (R1.4) Silty sand with granules and silty nodules; (R1.5) Coarse sand with gravel; (R1.6) Carbonate level (granular calcrete); (R1.7) Clayey sand with limestone; (R1.8) Sandy clay with bioturbation; and (R1.9) Organic sandy level.

4.2 Optically Stimulated Luminescence (OSL)

The samples were opened under a red light in the handling room. They were slightly disaggregated to obtain particles smaller than 150 μm. The samples were initially chemically treated for quartz, but they failed the OSL response test for quartz/feldspar [36]. This failure revealed a significant amount of feldspar, which would have skewed the results if

Fig. 2 Lithostratigraphic description of sedimentological profile excavated in the tank. OSL represents the sampling points for dating
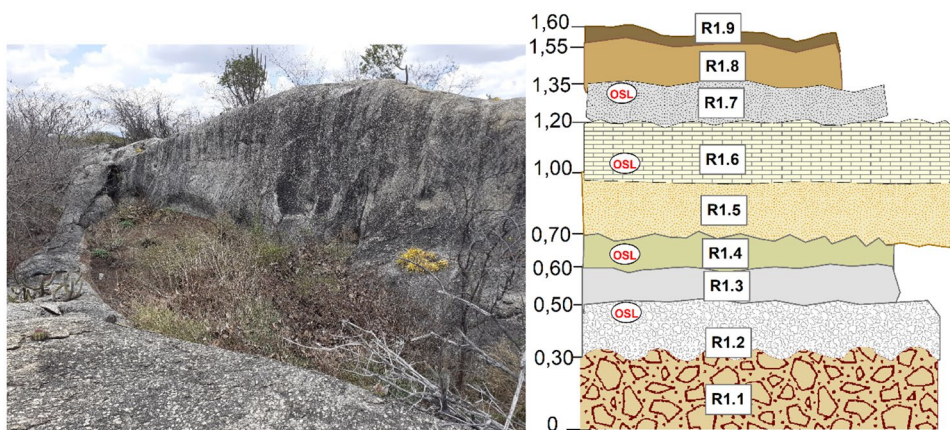
blue light stimulation were used. In response, the samples were treated to isolate the feldspar grains.

Afterward, the resulting fractions were chemically treated by immersion in a 10% HCl and 30% H_2O_2 solution, effectively removing carbonates and organic material. Each sediment sample was cleaned with acetone and dried at a controlled temperature of 50 °C in an oven for one hour. Then particle size classification (20–38 μm) was performed, and around 100 pellets were prepared.

The equivalent dose (De) for each pallet was established using the post-IR IR signal [39–42]. This procedure uses the Single Aliquot Regeneration - SAR protocol that measures sensitivity changes between consecutive measurement cycles, as indicated by the OSL response to a minor test dose [37, 38]. The corrected OSL ratio (regenerated OSL response divided by the OSL response to the fixed test dose - Ln/Tn) is projected to remain independent of previous dose or thermal treatments.

To confirm this, a specific regenerative dose is reiterated following exposure to varying higher doses. The ratio of the two regenerated sensitivity-corrected OSL responses, known as the recycling ratio, is then evaluated. Ideally, this ratio should be close to one [37]. Recycling ratios for all analyzed samples should ideally range between 0.90 and 1.10.

Furthermore, preheating the sample can result in the recovery of the OSL signal. To evaluate this effect, a 0 Gy regenerative dose step is added to the SAR protocol [37]. In this context, the luminescence signal should register as zero; this is referred to as the 'recuperated' luminescence signal. Any aliquots with grains showing a sensitivity-corrected recuperated signal exceeding 5% should be noted. The post-IR IR signal follows steps based on the SAR protocol [41, 42]: (1) Give regenerative dose (Di), (2) preheat at 250 ºC for 60 s, (3) IRSL measurements at 50 ºC for 100 s, (4) IRSL measurements at 225 ºC for 100 s (Li), (5) Give test dose (Dt), (6) Preheat (250 °C for 60 s), (7) IRSL measurements at 50 ºC for 100 s, (8) IRSL measurements at 225 ºC for 100 s (Ti), (9) IRSL measurements at 290 ºC for 40 s, (10) Return step 1.

The Lexyg smart OSL reader, equipped with infrared optical stimulation (200 mW/cm^2 and 410 nm filter), was used for these measurements. The pellets were irradiated within the reader using its internal $^{90}Sr/^{90}Y$ beta source, with a dose rate of approximately 0.1 Gy/s. Only the pellets that successfully passed all SAR protocol quality tests were used to calculate the equivalent dose. The dose recovery test ratio was consistent within 5%, recuperation ratios were consistently less than 5% and aliquots inconsistent with unity at 2 standard errors were excluded from the recovery test. These results were employed in determining De values and age calculations according to the Central Age Model [2, 43].

In the second step, the concentrations of radioisotopes, indicating the sediment's external radiation dose rate, were measured using a Canberra Eagle 5004 HPGe detector and a Canberra Eagle Plus multichannel analyzer. The sediments were dried at 50 °C for 24 h, disaggregated, and stored in plastic vials for a minimum of 30 days before measurement to ensure secular equilibrium, as cited in references 39 and 40. The water content of the sediments, both as-received and when water-saturated, was measured using Aitken's standard weight loss procedure. Since the site's current water content varies from the past, the ratio of the saturated to as-received water content was used to calculate the age of the sediments [44].

The internal dose calculation considers the effects of α and β particles and gamma radiation that arise from radioactive materials in the sample. Gamma rays, with a penetration power of 300 mm, typically surpass the sample's thickness, except for bricks. Therefore, their contribution to the internal dose rate calculation is ignored, leaving α and β particles as the primary contributors [44, 45].

For the gamma spectrometry calculation of uranium (U), thorium (Th), and potassium (K) content, a relatively large sample size is required. In cases where a large sample size is not available, as in feldspar grains from potassic sediment samples, the internal dose can be estimated with an assumed potassium content of $K = 12.5 \pm 0.5\%$ [45–49]. For this study, the contribution from internal beta activity is based on an effective potassium content of $12.5 \pm 0.5\%$ [46].

Lastly, each sample's age was calculated from the equivalent dose to the annual dose rate ratio at the site where the sample was procured.

The equivalent dose refers to the estimated absorbed radiation dose by grains, measured in Gy. The dose rate quantifies the total contribution from both internal and external radiation exposure, measured in Gy/kyr (grays per kilo year).

5 Results and Discussions

5.1 Optically Stimulated Luminescence - OSL

Table 1 presents the dating results for levels R1.2, R1.4, R1.6, and R1.7. This table includes the equivalent dose and annual dose rate for each sample. We collected all samples from a geographical coordinate of 8°10′51.3″ S 36°09′36.6″

Table 1 List of dated sediment samples with dose rates, equivalent dose, and age values

Sample	Depth (m)	Equivalent dose (Gy)	Annual dose rate (uGy/years)	Age years
R 1.7	1,35	34.0 ± 2.6	8895 ± 508	3832 ± 339
R 1.6	1,05	64.9 ± 2.6	$15{,}453 \pm 632$	4194 ± 223
R 1.4	0,65	52.4 ± 1.1	7406 ± 396	7078 ± 401
R 1.2	0.5	394 ± 17	8742 ± 487	$45{,}058 \pm 3093$

W. The radial plot and the IRSL growth curves of the samples R1.6 and R1.4 can be seen in Fig. 3.

The OSL dating results reveal three distinct deposition events in the tank's filling within the studied area. The first event occurred approximately 45,000 years ago at the base of the profile. The second event occurred around 7,000 years ago, and the third event occurred between 4,000 and 3,000 years ago at the top of the profile.

Calcrete formation, primarily from calcite cementation, was observed at both the base (45,000 years ago) and the top (4,000 years ago) depositions. These calcretes originate from pedogenesis [50–52].

According to Suguio [53], a paleosol is a soil that was formed in ancient geological times. It can be found either on the surface of the earth or buried underneath. As an example of a paleosol, the author cites the lateritic crust.

According to Retallack [54], paleosol refers to any soil created before the Holocene (before 11,000 BP) that is preserved in geological records, illustrating past environments. The pedogenetic calcretes at the base of the investigated profile in the tank situated in the Fazenda Nova district may represent one such paleosol.

Guerra and Guerra [55] posit that one method to detect a paleosol is by noting a darker subsurface horizon, potentially the A horizon, in locations such as a road cut. This darker layer may indicate soil buried by past sedimentation.

Calcretes are part of the pedocal group, usually linked with arid climates where limited water and scarce vegetation impede weathering processes. In these conditions, the sedimentary fill often holds a wealth of unmodified minerals from the bedrock, including calcium and other soluble minerals. Most of the soil, located close to the surface,
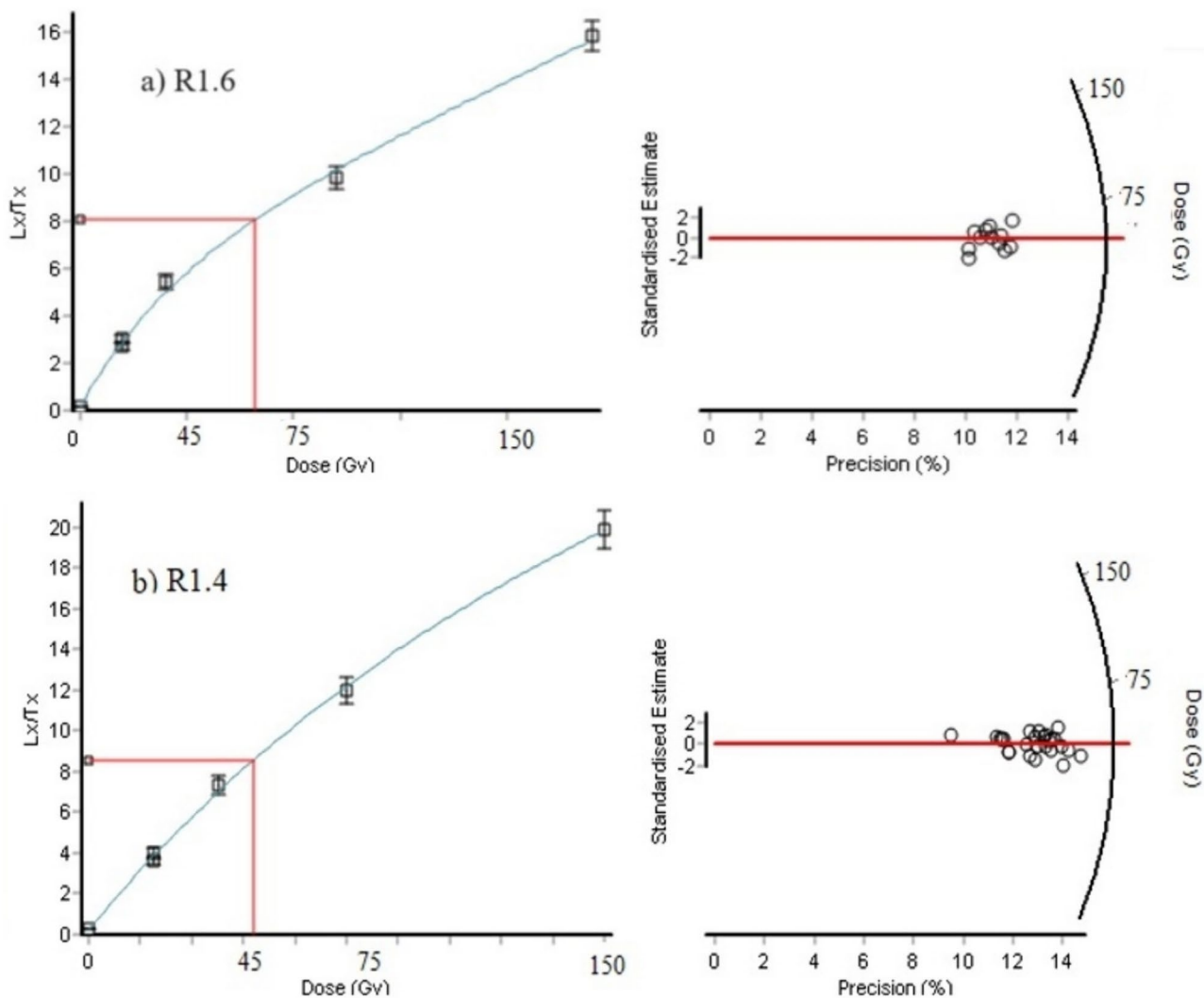
Fig. 3 Radial plot and the IRSL growth curves of **a** R1.6 and **b** R1.4 samples

experiences evaporation between periods of rainfall. This leads to the formation of nodules and concretions of calcium carbonate precipitates [56].

In his Master's thesis, "The Pleistocene mammals of Fazenda Nova, Brejo da Madre de Deus, Pernambuco: Taphonomic, Taxonomic, and Paleoenvironmental Aspects", Alves [57] examined the tank at Fazenda Icó, roughly 1 km from the tank assessed in this study. He discovered that:

"the tank deposit had four phases of sedimentary fill-ing by detrital flows, with the fossils being, mainly, in the second layer, a conglomerate with disarticulated bones and teeth whole and fragmented, arranged cha-otic, densely packed in rock (bone bed) with calcifer-ous cement (calcrete)" [57]

He also carried out the dating process for the teeth and calcrete cement. The teeth of Stegomastodon waringi discov-ered in the calcrete were dated using electron paramagnetic resonance (EPR), which revealed ages of $63,000 \pm 8,000$ and $60,000 \pm 9,000$. Meanwhile, the calciferous cement from the same layer was dated approximately 19,000 years BP using 14C dating. These results indicate that the cementation pro-cess occurred after the burial of the bones.

Listo et al. [58] conducted a study on sedimentary depo-sition in a pit, which was also investigated by Alves [57]. The team concluded that the deposits filling the weathering pits originated from gravitational sedimentation, particularly from debris flow, under torrential conditions. They found that the history of these records correlated with pedogenesis/morphogenesis cycles under different combinations of semi-aridity prevalent in the region.

The researchers used several methods to obtain these results. They analyzed depositional events and climate vari-ability, conducted a morphostratigraphic study, used OSL for dating, performed O18 isotope analysis on carbonate crust (calcrete), and undertook phytolith studies.

6 Conclusions

Two types of calcrete were discovered within the examined sedimentological profile: conglomeratic calcrete, which includes fragments of megafauna (R1.2), and granular cal-crete (R1.6). The conglomeratic calcrete was formed by exposing the top of the saprolite, depositing megafauna bone fragments, and then undergoing carbonate cementa-tion. This cementation process stemmed from the weath-ering of alluvial deposits from the porphyritic granite of the Fazenda Nova Pluton, taking place in times of tectonic stability typically seen in semi-arid to arid continental con-ditions. The weathering processes recorded at the sampled levels showed substantial cementation at the calcrete levels, evidenced by porochannels and bone fragments, suggesting

the cementation of sediments took place post-deposition. Illuviation and eluviation processes were detected via poro-channels, seen by mineral changes at their edges, indicating an upward/downward fluid movement within the profiles.

Declarations

References

1. O.B. Lian, R.G. Roberts, Quat. Sci. Rev. (2006). https://doi.org/10.1016/j.quascirev.2005.11.013
2. G.A.T. Duller, J. Quat. Sci. (2004). https://doi.org/10.1002/jqs.809
3. P. Mosca, Stud. Quat. (2019). https://doi.org/10.24425/sq.2019.126387
4. F.W.J. Cruz, S.J. Burns, I. Karmann, W.D. Sharp, M. Vuille, J.A. Ferrari, A stalagmite record of changes in atmospheric circulation and soil processes in the Brazilian subTropics during the Late Pleistocene. Quat. Sci. Rev. **25**, 2749–2761 (2006)
5. L.C.R. Pessenda, S.E.M. Gouveira, A.S. Ribeiro, P.E. de Oliveira, R. Areavena, Palaeogeogr. Palaeoclimatol. Palaeoecol. (2010). https://doi.org/10.1016/j.palaeo.2010.09.008
6. V.F. Novello, F.W. Cruz, M. Vuille, N.M. Stríkis, R.L. Edwards, H. Cheng, S. Emerick, M.S. de Paula, X. Li, E.S. Barreto, I. Karmann, R.V. Santos, Sci. Rep. (2017). https://doi.org/10.1038/srep44267
7. G. Utida, F.W. Cruz, R.V. Santos, A.O. Sawakuchi, H. Wang, L.C.R. Pessenda, R.L. Edwards, Quat. Sci. Rev. (2020). https://doi.org/10.1016/j.quascirev.2020.1066
8. M.F. Thomas, CATENA (2001). https://doi.org/10.1016/s0341-8162(00)00133-8
9. M.F. Thomas, CATENA (2004). https://doi.org/10.1016/s0341-8162(03)00111-59
10. D.N. Fonsêca, A.C.B. Corrêa, B.A.C. Tavares, D.B.R. de Lira, A.C.M. de Barros, A.C. Silva, D. Mützenberg, Earth Surf. Proc. Land. (2020). https://doi.org/10.1002/esp.4982
11. G.J. Retallack, Core concepts of paleopedology. Quater. Inter. **51**(52), 203–212 (1998)
12. A. Murray, L. Arnold, J.P. Buylaert, G. Guerin, J. Qin, A. Singhvi, R. Smedley, K. Thomsen, Nat. Rev. Methods Primers (2021). https://doi.org/10.1038/s43586-021-00068-5
13. S.A. Mahan, T.M. Rittenour, M.S. Nelson, N. Ataee, N. Brown, R. DeWitt, J. Durcan, M. Evans, J. Feathers, M. Frouin, G. Guérin, M. Heydari, S. Huot, M. Jain, A. Keen-Zebert, B. Li, G.I. López, C. Neudorf, N. Porat, K. Rodrigues, A.O. Sawakuchi, J.Q.G. Spencer, K. Thomsen, Guide For Interpreting and reporting luminescence dating results. GSA Bull. **135**, 1480–1502 (2023)

14. J. Wallinga, J. Sevink, J.M. van Mourik, T. Reimann, Luminescence dating of soil archives, in *Reading the Soil Archives*. ed. by J.M. van Mourik, J.J.M. van der Meer (Elsevier, 2019), pp.115–162

15. J.A. Durcan, Luminescence Dating. Encyclopedia of Geology (2021). https://doi.org/10.1016/b978-0-12-409548-9.12105-0

16. J.K. Feathers, Meas. Sci. Technol. (2003). https://doi.org/10.1088/0957-0233/14/9/302

17. R.R. Carvalho, V.K. Asfora, W.A. Lima de Moura, J.A. Barbosa, G.M. Silva Ramos, V.H.M.L. Neumann, J South Am Earth Sci (2024). https://doi.org/10.1016/j.jsames.2024.104798

18. G. Hütt, I. Jaek, J. Tchonka, Optical dating: K-feldspars optical response stimulation spectra. Quat. Sci. Rev. **7**, 381–385 (1988)

19. progress in luminescence dating of sediments, O. B. L., Lian, R.G. Roberts, Dating the Quaternary. Quat. Sci. Rev. **25**, 2499–2468 (2006)

20. G.A.T. Duller, Equivalent dose determination using single aliquots. International Journal of Radiation Applications and Instrumentation. Int J Radiat Appl Inst Part D Nucl Track Radiat Meas **18**, 371–378 (1991)

21. M. Lamothe, S. Balescu, M. Auclair, Natural IRSL intensities and apparent luminescence ages of single feldspar grains extracted from partially bleached sediments Radiat. Meas. **23**, 555–562 (1994)

22. B. Li, R.G. Roberts, Z. Jacobs, Quat. Geochronol. (2013). https://doi.org/10.1016/j.quageo.2013.03.006

23. B. Li, S. H. LI,. J. Phys. D: Appl. Phys. (2008). https://doi.org/10.1088/0022-3727/41/22/225502

24. B. Li, S.H. Li, Luminescence dating of K-feldspar from sediments: A protocol without anomalous fading correction. Quat. Geochronol. **6**, 468–479 (2011)

25. A.C.B. Corrêa, B.A.C. Tavares, K.A. Monteiro, L.C.S. Cavalcanti, D.R. Lira, Megageomorfologia e Morfoestrutura do Planalto da Borborema. Rev. Inst. Geo. **31**, 35–52 (2010)

26. H.G.S. Santos, P.K. Jacomine, L.H.C. Anjos, V.A. Oliveira, J.F. Lumbreras, M. R. Coelho, J.A. Almeida, J.C. Araújo Filho, J.B. Oliveira, T.J.F. Cunha, Sistema brasileiro de classificação de solos, 5nd edn. (Embrapa, Brasília) 356 (2018)

27. F.F.M. Almeida, Y. Hasui, *O Pré-Cambriano do Brasil* (São Paulo, Edgard Blucher, 1984), p.378

28. G. Mariano, J. M. R Silva, P.B. Correia, S.P. Neves, A.F. Cabral, F.M.V. Silva, I.T. Chagas, T.S. Miranda, S.F.Oliveira, B.S. Freire, Nota Explicativa da Folha Belo Jardim (SC.24-X-B-III) 1:100.000 (CPRM, Brasil) 80 (2008)

29. E.J. Santos, O complexo granítico de Lagoa das Pedras: acresção e colisão na região de Floresta (PE), Província Borborema. [Doctoral Thesis]. São Paulo: Instituto de Geociências, Universidade de São Paulo – USP, 220 (1995). https://doi.org/10.11606/T.44.1995.tde-28102015-094036

30. E.J. Santos, V.C. Medeiros, Constraints from granitic plutonism on proterozoic crustal growth of the transverse zone, Borborema Province. NE Brazil. Rev. Bras. Geoc. **29**, 73–84 (1999)

31. S.P. Neves, A.M.B. Araújo, P.B. Correia, G. Mariano, J. Struct. Geol. (2003). https://doi.org/10.1016/S0191-8141(02)00003-2

32. S.P. Neves, S.C. Melo, C.A.V. Moura, G. Mariano, J.M. Rangel Da Silva, Int. Geol. Rev. (2004). https://doi.org/10.2747/0020-6814.46.1.52

33. S.P. Neves, O. Bruguier, A. Vauchez, D. Bosch, J.M.R. Silva, G. Mariano, Precambrian Res. (2006). https://doi.org/10.1016/j.precamres.2006.06.005

34. S.P. Neves, G. Mariano, J. Struct. Geol. (1999). https://doi.org/10.1016/S0191-8141(99)00097-8

35. S.P. Neves, A. Vauchez, G. Feraud, Precambrian Res. (2000). https://doi.org/10.1016/S0301-9268(99)00026-1

36. G.A.T. Duller, Radiat. Meas. (2003). https://doi.org/10.1016/S1350-4487(02)00170-1

37. A.S. Murray, A.G. Wintle, Radiat. Meas. (2000). https://doi.org/10.1016/S1350-4487(99)00253-X

38. A.S. Murray, A.G. Wintle, Radiat. Meas. (2006). https://doi.org/10.1016/j.radmeas.2005.11.001

39. K.J. Thomsen, A.S. Murray, M. Jain, L. Bøtter-Jensen, Radiat. Meas. (2008). https://doi.org/10.1016/j.radmeas.2008.06.002

40. P. Morthekai, M. Jain, A.S. Murray, A.S. Thomsen, L. Bøtter-Jensen, Radiat. Meas. (2008). https://doi.org/10.1016/j.radmeas.2008.02.019

41. J.P. Buylaert, A.S. Murray, K.J. Thomsen, M. Jain, Radiat. Meas. (2009). https://doi.org/10.1016/j.radmeas.2009.02.007

42. M. Jain, C. Ankjaergaard, Radiat. Meas. (2011). https://doi.org/10.1016/j.radmeas.2010.12.004

43. R.F. Galbraith, R.G. Roberts, G.M. Laslett, H. Yoshida, J.M. Olley, Optical dating of single and multiple grains of quartz from Jinmium rock shelter, northern Australia. Part I, experimental design and statistical models. Archaeometry **41**, 339–364 (1999)

44. M.J. Aitken, *Thermoluminescence dating* (Academic Press, London, 1985), p.351

45. W. Weida, Sci. China Technol. Sci. (2008). https://doi.org/10.1007/s11431-008-0022-z

46. D.J. Huntley, M.R. Baril, The K content of the K- feldspars being measured in optical dating or in thermoluminescence dating. Ancient TL. **19**, 43–46 (1997)

47. D.J. Huntley, R.G.V. Hancock, The Rb contents of the K- feldspars being measured in optical dating. Ancient TL. **19**, 43–46 (2001)

48. H. Zhao, S.H. Li, Internal dose rate to K-feldspar grains from radioactive elements other than potassium. Radiat. Meas. (2005). https://doi.org/10.1016/j.radmeas.2004.11.004

49. B. Li, S.H. Li, J. Phys. D Appl. Phys. (2008). https://doi.org/10.1088/0022-3727/41/22/225502

50. A.M. Alonso-Zarza, Earth Sci. Rev. (2003). https://doi.org/10.1016/S0012-8252(02)00106-X

51. E. Maoski, Gênese dos calcretes da Formação Marília no Centro-Oeste Paulista e Triângulo Mineiro, Bacia Bauru. [Master's Dissertation] Curitiba: Setor de Ciências da Terra, Universidade Federal do Paraná - UFPR, p. 94 (2012). https://acervodigital.ufpr.br/handle/1884/27326

52. P.B. Adler, L.F. De Ros, K.L. Mansur, A.L. Ferrari, Thjbdva asvafnugav. Pesq. Geoc. (2017). https://doi.org/10.22456/1807-9806.78274

53. K. Suguio, *Geologia do Quaternário e mudanças ambientais. Passado + Presente = Futuro* (São Paulo, Paulo's Editora, 1999), p.366

54. G.J. Retallack, *Soils of the past: an introduction to paleopedology* (Blackwell Science, Oxford, 2001), p.404

55. A.T. Guerra, A.J.T. Guerra, *Novo Dicionário Geológico-Geomorfológico, 3ed* (Bertrand. Brasil, Rio de Janeiro, 2003), p.652

56. F. Press, J. Grotzinger, T.H. Jordan, *Para Entender a Terra* (Bookman, Porto Alegre, 2006), p.656

57. R.S. Alves, Os mamíferos de fazenda Nova, Brejo da Madre de Deus, Pernambuco: aspectos tafonômicos, taxonômicos e paleoambientais. [Master's dissertation] Recife: Programa de Pós-Graduação em Geociências, Universidade Federal de Pernambuco – UFPE 127 (2007). https://repositorio.ufpe.br/handle/123456789/6492

58. D.G.S. Listo, R.F.T.M. Balder, A.C.B. Corrêa, D.A.M.C. Ramos, M.R. Calegari, Quat. Int. (2023). https://doi.org/10.1016/j.quaint.2022.10.004